An inherently fault tolerant control of sodium cooled fast reactors and its stability analysis using particle swarm optimization

Muthuraj T[1,2*], John Arul[1,2], Piyush V. Surjagade[3],
Vineet Vajpayee[4], V. Becerra[3], J. Deng[3]

[1]Homi Bhabha National Institute, Mumbai, India.
[2]Indira Gandhi Centre for Atomic Research, Kalpakkam, India.
[3]School of Built Environment, Engineering and Computing,
Leeds Beckett University, Leeds, LS6 3QR, United Kingdom.
[4]Department of Automatic Control and Systems Engineering,
The University of Sheffield, UK.

Abstract

In this study we propose a simple, yet inherently fault-tolerant and robust controller utilizing a combination of both feedforward and feedback control schemes. Feedback controllers are known to be robust, but feedforward controllers can be reliable in the context of safety as they can be less dependent on measurements. Though, many combined feedforward and feedback controllers have been proposed in the literature, to the best of our knowledge a controller tolerant to the failure of power feedback signal is nowhere demonstrated. In this scheme, major corrections are effected by a model predictive forward control unit, while bounded uncertain part is corrected by a feedback control unit. The feedforward control is implemented using the inverse equations of the nuclear reactor point kinetics model. The bounded error control is effected by a simpler limited Proportional-Integral-Derivative (PID) feedback controller. Stability analysis of the controller is carried out numerically by Lyapunov's direct method with the help of Particle Swarm Optimization (PSO) technique. The proposed controller (referred to as Inverse Dynamics Corrected Control (IDCC)), is studied for reactor power control with model error plus uncertainty and a principal feedback signal failure case (i.e. power sensor failure). It is shown that the IDCC has excellent load tracking performance for a challenging demand profile with model error, in comparison to Sliding Mode Controller (SMC) and a manually tuned PID controller. For the loss of principal feedback signal case, there is a trade off between the tracking performance of IDCC and safety aspects. While both PID and SMC drive the reactor power to unsafe levels, IDCC maintains the reactor power within a safer bound.

Highlights

- A conceptually new controller tolerant to failure of the principal feedback signal, has been designed by combining feedforward and feedback control schemes.
- The controller's stability is demonstrated by Lyapunov's direct method with the particle swarm optimization algorithm.
- The controller is shown to be fault tolerant, robust and have very good power tracking performance by comparison with PID and sliding mode controllers.
- Many case studies have been performed to illustrate the performance of the controller.

Keywords

Fault tolerant control, particle swarm optimization, nonlinear stability analysis, feedforward control, feedback control.

1 Introduction

Nuclear energy is one of the most dependable and efficient sources of energy. It can play a significant role in rapidly reducing the dependence on fossil fuels, to mitigate the climate crisis. At present nuclear power plants (NPP) are employed to meet about 20% of the global electric power demand, which is expected to grow in the coming decades [1, 2]. In this context, increasing number of reactors mean that reliability and safety of the reactors need to be further strengthened to keep the number of unexpected events from increasing and impacting public opinion. Therefore, the present generation of nuclear reactors are being designed with enhanced safety, compared to previous generation reactors [3, 4]. The first line of defense in depth in nuclear safety philosophy is to prevent abnormal operation and failures by inherently safe design and use of high quality components. The second line of defense in depth envisages effective control and protection systems. This requires the design of reactor control systems to be inherently stable, robust and to have fault tolerant and fail safe features [5]. In this paper, we address the inherent fault tolerant characteristics of nuclear reactor power control systems. Though the sensors and other components of the control system are designed with state-of-the-art technology and industrial strength, highly reliable hardware, verified and validated software, it is important to incorporate to the extent feasible, tolerance to faults and even likely failures, inorder to ensure robustness of the safety design [6].

Fault tolerance implies continued functioning of the control system, possibly with degraded performance under a single failure in either input, actuators, or components of the control system [7]. There have been several studies in the literature to design fault tolerance using component redundancy, fault detection and correction methods [8]. However, this approach would entail increased cost and complexity of the control system and associated instrumentation. In this context, an approach that is simple and uses inherently fault tolerant characteristics of well-known control schemes would be advantageous on several counts. Less complexity would translate to better reliability of the control system, coupled with less effort required for verification and validation excercises. Further regulatory approval of well-known schemes would be easier to obtain compared to novel but complex methods.

The subject of this paper is to investigate a reactor power control scheme, that could withstand critical failures when compared to conventional controllers. The most popular and simple feedback controller often used is the Proportional-Integral-Derivative (PID) controller [9, 10] which adds the input to the system by proportional, time integral, and time derivative of relative error of the output power to demand power. PID can have disadvantages like poor control for nonlinear systems and not inherently fault tolerant to component failures. A better performing controller, proposed in the literature for reactor control [11] is the Sliding Mode Controller (SMC) and its variants, which are capable of handling plant's model error because of their inherent error tolerance behavior. A number of robust non-linear feedback controllers have been developed by researchers to control reactor power such as Linear Quadratic Control (LQR), Model Predictive Controller (MPC), Fuzzy logic PID controller, adaptive control, neural network-based controllers, etc [12, 13, 14] to name a few.

Most of the above controllers make use of feedback effects to achieve error reduction but can overdrive the system, in case of a failure in the measurement subsystem as happened in the Boeing 737 Max accident [15]. Here, the immediate cause of the accident is a failure in the angle of attack sensor, causing the control system to increase the pitch and eventual aircraft stall. In nuclear reactors, it is essential to ensure that, at no point, the control system introduces a large amount of positive reactivity. If this is done by limiting the control reactivity directly, the control system performance will be degraded. Therefore, in the proposed scheme we combine the inherent error-correcting capability of feedback controllers with a feedforward control. The feedforward control predicts the required reactivity input a priori from the demand power. However, as the feedforward control cannot handle model error and uncertainties, a limited feedback controller is added to control the deviations from model prediction. The feedforward model is implemented by means of an inverse dynamics model, which outputs the net reactivity required for a given power demand. For implementing this scheme in situations where the dynamics are not invertible, the forward model can be used iteratively, as in model predictive control. In short, here the first estimate of reactivity required for the reactor to achieve the desired power, is obtained from the inverse point kinetics equation and only the limited correction required for tight control is obtained from PID control.

There have been few good studies in the literature combining feedforward and feedback controllers for the robust power tracking performance of NPPs [16, 17]. Though these controllers are very good at handling model error and external disturbances, the power signal failure case, which is a plausible scenario having an adverse effect on safety, is not studied. All the above control techniques, though, can reject errors introduced into the system, they are not fault tolerant [18]. In an interesting design of

a robust and resilient control system [19], a finite state machine is used to smoothly switch between a robust controller for normal operation and an L-1 adaptive controller for resilient control under abnormal conditions. The controller is studied for loss of coolant accident and loss of flow accident, but the power signal failure case is not studied explicitly. And also the controller requires fault diagnosis and switching systems, which increase the complexity of the system.

It is to be noted here that, in the proposed design any other linear feedback controller can be used in place of the PID controller as handling nonlinearity and fault tolerance is achieved by the feedforward part of the controller. The advantage of the present control system is that, it is easy to implement and verify. The reactivity added by the PID is always limited, yet large corrections can come from the feedforward model. This scheme ensures that the controller does not command large reactivity additions because of any error or failure in the power measurement subsystem.

The structure of the paper is as follows. The proposed Inverse Dynamics Corrected by PID Control (IDCC) strategy is explained in section 2. The stability analysis of the proposed controller is carried out in section 3. The performance of the proposed controller is studied and reslts presented for cases of challenging demand profiles with uncertainty and a component failure case, in section 4. The performance of the IDCC is compared with SMC and an empirically tuned PID controller. Results and conclusions are presented in section 5.

2 Inverse Dynamics Corrected Control (IDCC)

Conceptually the control approach adopted in the IDCC is as follows. For controlling a system along the desired trajectory, it would be prudent to apply the known or a priori estimated control actions for any large changes required in the system trajectories. Any tracking error, occurring due to uncertainties can be corrected by feedback control, as it would be difficult to calculate such effects in advance. Accordingly, the control method proposed has two major units, as shown in Figure (1). One is a feedforward unit and another one is a feedback unit. In the feedforward unit, an inverse dynamics model is used to estimate the reactivity to be added by control rods to achieve the required power. The Inverse Point Kinetics Equation (IPKE) module generates the net reactivity ρ corresponding to the demand power P_d (normalized). The reactivity feedback estimator module estimates the thermal reactivity feedback ρ_f, using inputs of demand power P_d, coolant inlet temperature T_{in} and coolant mass flow rate Q. The estimated ρ_f is subtracted from the net reactivity estimated by the IPKE module, to get the control rod reactivity ρ_{cr}. Since it is not possible to correct any small deviations of the actual power, arising from model error or uncertainty, by the feedforward control, a reactivity limited PID feedback unit is added for the tight power control. In the feedback unit, the output power is measured by an observer (basically a power sensor) and the deviation signal is given to the PID module. The PID output is constrained by a limiter and the PID correction $\widetilde{\rho}_{pid}$ is added to ρ_{cr} to arrive at the corrected control rod reactivity $\widetilde{\rho}_{cr}$ which is finally applied as control input to the plant. Because of the feedforward unit, the reactivity added by the feedback PID controller unit can be limited to a value less than one β. This is expected to keep the period of the transients reasonably long and magnitude manageable thereby, contributing to the plant safety. In the proposed scheme, the dependence of the controller on measured values is minimized as T_{in}, mass flow rate of the coolant and P are the only values measured. The controller is tolerant to measurement errors of power and since T_{in} and Q are usually kept constant in sodium cooled reactors, the measurement of these two parameters can be validated easily, making them fault tolerant.

2.1 Model of nuclear reactor power and primary system temperature

For this study, the dynamics of the nuclear reactor power is represented by a set of coupled first order ordinary differential equations, called reactor point kinetics equations, wherein it is assumed that the spatial flux shape is independent of time and time dependence of flux is represented by an amplitude function. This model is valid for tightly coupled cores [20]. Even though there are many advanced model of reactors like multi-point kinetics [21] and other nonlinear model [22], we have chosen very basic and efficient model of the reactor to demonstrate the fault tolerant aspect of the proposed controller. In this model, the change in reactor power and neutron precursor concentration can be represented as,

$$\frac{dP(t)}{dt} = \left(\frac{\rho(t) - \beta}{\Lambda}\right) P(t) + \sum_{i=1}^{6} \lambda_i C_i(t) + S \tag{1}$$

$$\frac{dC_i(t)}{dt} = \frac{\beta_i}{\Lambda} P(t) - \lambda_i C_i(t) \quad ; i = 1, 2, \ldots, 6 \tag{2}$$

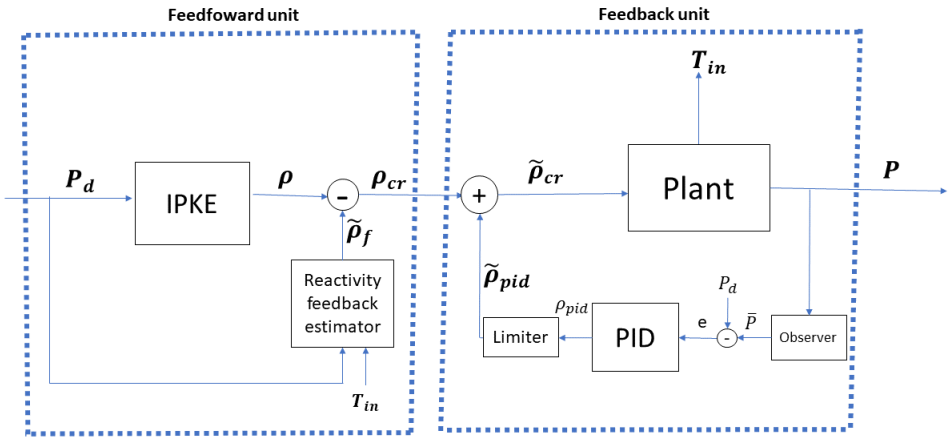

Figure 1: Block diagram for IDCC controller.

Where, P(t) is reactor power at time t, $\rho(t)$ is the net reactivity at time t, $C_i\,(t)$ is proportional to the concentration of i^{th} group delayed neutron precursors, β_i is i^{th} group delayed neutron fraction, λ_i is decay constant of i^{th} group delayed neutron precursors, β is the effective delayed neutron fraction, S is proportional to the external neutron source strength, Λ is the mean generation time of neutrons.

The thermal hydraulics model consists of a lumped system, as shown in the Figure(2). It is represented by a set of differential equations for fuel, cladding and coolant temperatures, as listed below.

$$\frac{dT_1(t)}{dt} = a_1 P(t) - b_1 T_1(t) + b_1 T_2(t) \tag{3}$$

$$\frac{dT_2(t)}{dt} = a_2 T_1(t) - (a_2 + b_2) T_2(t) + \frac{b_2}{2} T_3(t) + \frac{b_2}{2} T_{in} \tag{4}$$

$$\frac{dT_3}{dt} = a_3 T_2(t) - \left(b_3 + \frac{a_3}{2}\right) T_3(t) + \left(b_3 - \frac{a_3}{2}\right) T_{in} \tag{5}$$

where,

$$a_1 = \frac{1}{m_f C_{pf}}; \qquad b_1 = \frac{h_{fw} A_{fw}}{m_f C_{pw}};$$

$$a_2 = \frac{h_{fw} A_{fw}}{m_w C_{pw}}; \qquad b_2 = \frac{h_{wc} A_{wc}}{m_w C_{pw}};$$

$$a_3 = \frac{h_{wc} A_{wc}}{m_c C_{pc}}; \qquad b_3 = \frac{u}{m_c C_{pc} H};$$

a_i, b_i are thermal coefficients involving heat capacity and heat transfer constants. m_f, m_w, m_c are mass of fuel, clad and coolant respectively. C_{pf}, C_{pw}, C_{pc} are specific heat capacity of fuel, clad and coolant respectively. A_{fw} is area between fuel and clad. A_{wc} is area between clad and coolant. T_1, T_2, T_3 are the fuel, clad and coolant outlet temperatures respectively. The schematic of a lumped thermal hydraulics model of the reactor is shown in Figure (2) .

The average coolant temperature $\bar{T_3}$ is given by

$$\bar{T_3} = \frac{T_3 + T_{in}}{2} \tag{6}$$

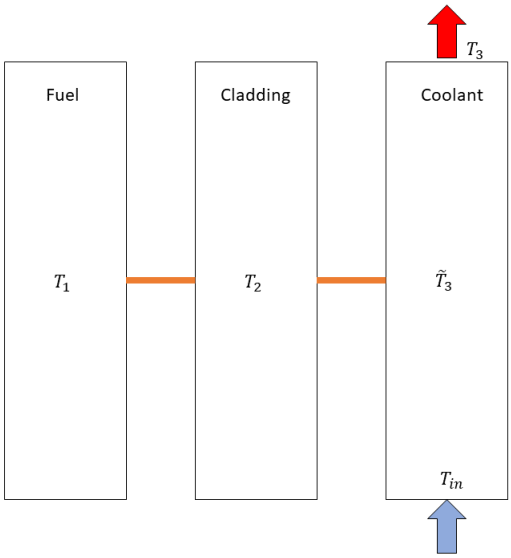

Figure 2: Lumped thermal hydraulics model of the reactor

The time dependent net reactivity is given by

$$\rho(t) = \rho_{cr}(t) + \rho_f(t) \tag{7}$$

Thermal feedback reactivity is given by

$$\rho_f(t) = \sum_i \alpha_i \Delta T_i \qquad i = 1, 2, 3 \tag{8}$$

$$\Delta T_i = T_i - T_i^{ref}$$

where, T_{in} is the reactor coolant inlet temperatures, $\rho_{cr}\,(t)$ is control rod reactivity at time t. $T_1^{ref}, T_2^{ref}, T_3^{ref}$ are reference temperatures of fuel, cladding and core respectively, $\alpha_1, \alpha_2, \alpha_3$ are the feedback reactivity coefficients of fuel, cladding and coolant respectively.

The values of the parameters corresponding to a typical medium sized Sodium-cooled Fast Reactor (SFR) are listed below in Table (1).

Parameter	**Unit**	**Value**
$\lambda_1, \lambda_2, \lambda_3$ $\lambda_4, \lambda_5, \lambda_6$	s^{-1}	0.0129, 0.0312, 0.1344, 0.3448, 1.3925, 3.753
$\beta_1, \beta_2, \beta_3,$ $\beta_4, \beta_5, \beta_6$	-	$8.246 \times 10^{-5}, 7.6817 \times 10^{-5}, 6.6926 \times 10^{-5},$ $1.2849 \times 10^{-5}, 5.7615 \times 10^{-5}, 1.7213 \times 10^{-5}$
β	-	3.553×10^{-3}
Λ	s	0.4×10^{-6}
a_1	$^\circ C J^{-1}$	362.161
a_2, a_3, b_1, b_2, b_3	s^{-1}	0.5579, 3.2088, 0.2608, 3.107, 6.5
$T_{1ref}, T_{2ref}, T_{3ref}$	$^\circ C$	1200, 700, 397
$\alpha_1, \alpha_2, \alpha_3$	$^\circ C^{-1}$	-1.0×10^{-5}, -1.0×10^{-5}, -1.0×10^{-5}
S	Ws^{-1}	0

Table 1: Values of the parameters used in the study

2.2 Feedforward control module

For the control problem, a reference (demand) power is known and from that, the corresponding net reactivity can be generated by means of the IPKE [23]. This equation relates the net reactivity to the demand power, and can be derived by integrating equation (2) and substituting back into equation (1)

as given below [24].

$$\rho(t) = \beta + \frac{\Lambda}{P_d(t)}\frac{dP_d(t)}{dt} - \frac{1}{P_d(t)}\left[P_d(0)\sum_{i=1}^{6}\beta_i e^{-\lambda_i t} + \int_0^t \sum_{i=1}^{6}\lambda_i\beta_i P_d(t')e^{-\lambda(t-t')}dt'\right] - \frac{\Lambda}{P_d(t)}S \tag{9}$$

where $\rho(t)$ is the net reactivity corresponding to the demand power $P_d(t)$ in terms of relative power at time t. Since the system has thermal feedback, it is required to estimate fuel, cladding and coolant temperatures to predict the feedback reactivity and from that the reactivity to be added by the control rods. This in turn requires the measured values of power and temperatures. Normally, in sodium cooled fast reactors, apart from power, only coolant inlet T_{in} and outlet temperature T_3 and coolant mass flow rate Q are measured. T_{in}, Q and P are sufficient to estimate the fuel, cladding and coolant average temperatures using the following set of equations. However, in the equations the measured power P is replaced by demand power P_d and $\check{T}_1, \check{T}_2, \check{T}_3$ are the estimated temperatures of fuel, cladding and coolant.

$$\frac{d\check{T}_1}{dt} = a_1 P_d(t) - b_1\check{T}_1(t) + b_1\check{T}_2(t) \tag{10}$$

$$\frac{d\check{T}_2}{dt} = a_2\left(\check{T}_1(t) - \check{T}_2(t)\right) - b_2\left(\check{T}_2(t) - \check{T}_3(t)\right) \tag{11}$$

$$\frac{d\check{T}_3}{dt} = a_3\left(\check{T}_2(t) - \check{T}_3(t)\right) - b_3\left(T_3(t) - T_{in}\right) \tag{12}$$

The estimated temperature feedback reactivity is given by,

$$\widetilde{\rho}_f(t) = \sum_i \alpha_i \Delta\check{T}_i(t) \qquad i = 1,2,3 \tag{13}$$

$$\Delta\check{T}_i(t) = \check{T}_i(t) - T_i^{ref}$$

The approximate control rod reactivity estimate is given by,

$$\rho_{cr}(t) = \rho(t) - \widetilde{\rho}_f(t) \tag{14}$$

This reactivity, if added by the control rods, would bring the reactor power very near the demand power, but without corrections required from uncertainties. The feedback correction is discussed in the next section.

2.3 Feedback control module

The implementation of PID controller to get the corrected control rod reactivity is as follows,

$$\widetilde{\rho}_{cr}(t) = \rho_{cr}(t) + \widetilde{\rho}_{pid}(t) \tag{15}$$

where,

$$\widetilde{\rho}_{pid}(t) = L\left(\rho_{pid}(t)\right) \tag{16}$$

And,

$$\rho_{pid}(t) = k_p e(t) + k_d\frac{d}{dt}e(t) + k_i\int_{-\infty}^{t} e(t')dt' \tag{17}$$

$$e(t) = P_d(t) - \widetilde{P}(t) \tag{18}$$

where, $\rho_{cr}(t)$ is the approximate control rod reactivity at time t (estimated in the feedforward module), P_d is demand power, $\widetilde{P}(t)$ is the measured power, $\widetilde{\rho}_{cr}$is corrected control rod reactivity, $\widetilde{\rho}_{pid}$ is reactivity correction from PID, e(t) is the error between the measured power and demand power at time t, k_p, k_d, k_i are PID parameters.

The reactivity correction through the PID is limited by a function,

$$L(x) = x; \quad when - B \le x \le B \quad else \quad L(x) = sign(x)\min(|x|, B) \tag{19}$$

Typically, B is set at about $\beta/10$. The PID parameters were tuned manually and are as follows,

$$k_p = 1.0\times10^{-4};\ k_d = 1.0\times10^{-5};\ k_i = 4.0\times10^{-4}$$

3 Stability analysis of IDCC

3.1 Lyapunov's stability theorem

The nonlinear stability of IDCC is analysed by using Lyapunov direct method. According to the Lyapunov stability theorem [25], for a given nonlinear autonomous dynamical system,

$$\dot{\mathbf{X}} = f(\mathbf{X}) \tag{20}$$

$$f(0) = 0$$

where, $\mathbf{X}$ is state vector and 0 is the equilibrium point of the system. If there exists a function $V(\mathbf{X}) : \mathbb{R}^n \to \mathbb{R}$, which satisfying the following criteria,

$$V(\mathbf{X}) > 0; \qquad \mathbf{X} \in \mathbb{R}^n - \{0\} \tag{21}$$

$$\dot{V}(\mathbf{X}) < 0; \qquad \mathbf{X} \in \mathbb{R}^n - \{0\} \tag{22}$$

$$V(\mathbf{0}) = \dot{V}(\mathbf{0}) = 0; \tag{23}$$

Then the system is asymptotically stable (eventually reaches equilibrium point after a perturbation) in the given domain $\mathbb{D} \subseteq \mathbb{R}^n$. Where $\mathbb{R}$ is the set of real numbers and n is the number of state variables of the dynamical system.

In simple words, the function must be positive definite for all values in the domain of the state variables, except at zero and time derivative of the function must be negative definite for all values in the domain $\mathbb{D}$ of state variables except at zero. Such a function is called a *Lyapunov function*, and if such a function exists, then the system is asymptotically stable with respect to that particular equilibrium point in the given domain $\mathbb{D}$.

The Lyapunov function candidate, to investigate the nonlinear stability of IDCC is

$$V = \frac{1}{2}e^2 \tag{24}$$

Where, $e = P_d - P$. Using error as Lyapunov function is the traditional approach for designing the control algorithm of controllers like sliding mode control, adaptive control, etc,.
The time derivative of the Lyapunov function is give by,

$$\dot{V} = e.\dot{e} \tag{25}$$

which is,

$$\dot{V} = (P_d - P)(\dot{P}_d - \dot{P})$$

For the demonstration purpose, let us assume the demand power P_d= a constant.The time derivative of the power $\dot{P}$ is given by equation (1).

$$\frac{dV}{dt} = -(P_d.\dot{P} + P.\dot{P}) \tag{26}$$

If the equation (26) is negative definite in the domain $\mathbb{D}$ where n is number of state variables of the dynamical system, then the system is asymptotically stable in that domain $\mathbb{D}$.
The negative definite characteristics of equation (26) is investigated, by numerically finding the maxima of the function. If the maxima of the function $\dot{V}$ is negative definite, then we can assume that entire function is negative for all values in the domain D. Now the problem becomes an optimization problem, which can be solved by any one of the robust global optimizing algorithms since time derivative of V is the function of 10 variables. The optimizer chosen to solve the problem is Particle Swarm Optimization (PSO) because of its simplicity and global search optimization capability.

A program has been written in python, which incorporates PSO algorithm for finding maxima of function $\dot{V}$.

3.2 Particle Swarm Optimisation:

Particle swarm optimization is one of the famous and effective optimizer which is used for finding maxima or minima of any cost function. The PSO algorithm for finding maxima of the time derivative of Lyapunov function is shown in Figure (3).

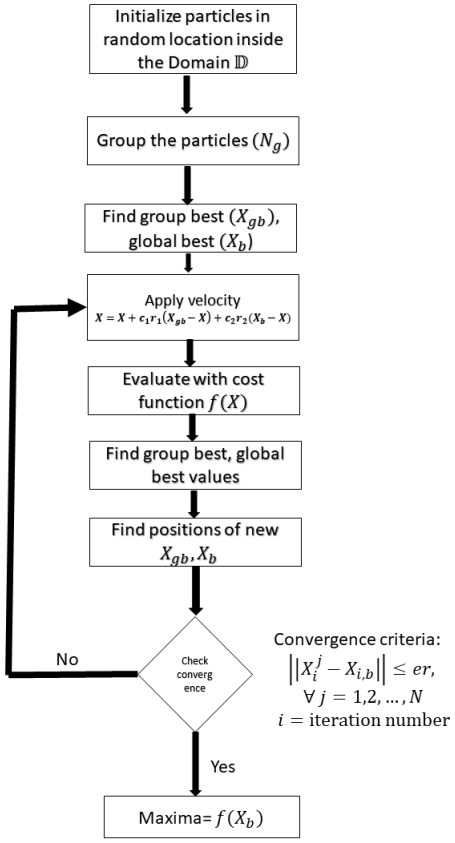

Figure 3: Flow chart of PSO algorithm

The flowchart of the algorithm is explained as follows. For the simulation, N number of particles are chosen. Each particle is allocated randomly over the domain $\mathbb{D}$ of the state space. The particles are grouped in equal size over the state space into N_g groups. One of the particles from each group is chosen as the best value X_{gb} (maxima) and global best X_b is chosen as best of $\{X_{gb}\}$. Each particle is moved according to the instruction for the velocity function v [26].

$$X_{i+1} = X_i + v_i \tag{27}$$

where,

$$v_i = c_1 r_1 (X_{gb}^i - X_i) + c_2 r_2 (X_b^i - X_i) \tag{28}$$

Where, X_i is the position vector of particles in i^{th} iteration, X_{gb}^i is the corresponding group best position and X_b^i is the corresponding global best position. c and r are acceleration coefficients, which take values in the range [0,1]. c_1 & c_2 are fixed and r_1 & r_2 are varying randomly in each iteration. Once the velocity function is applied, each particle is displaced towards group best and global best position, in a small step. The displacement of the particles towards the maxima of the cost function due to the computed velocity is depicted in Figure(4).

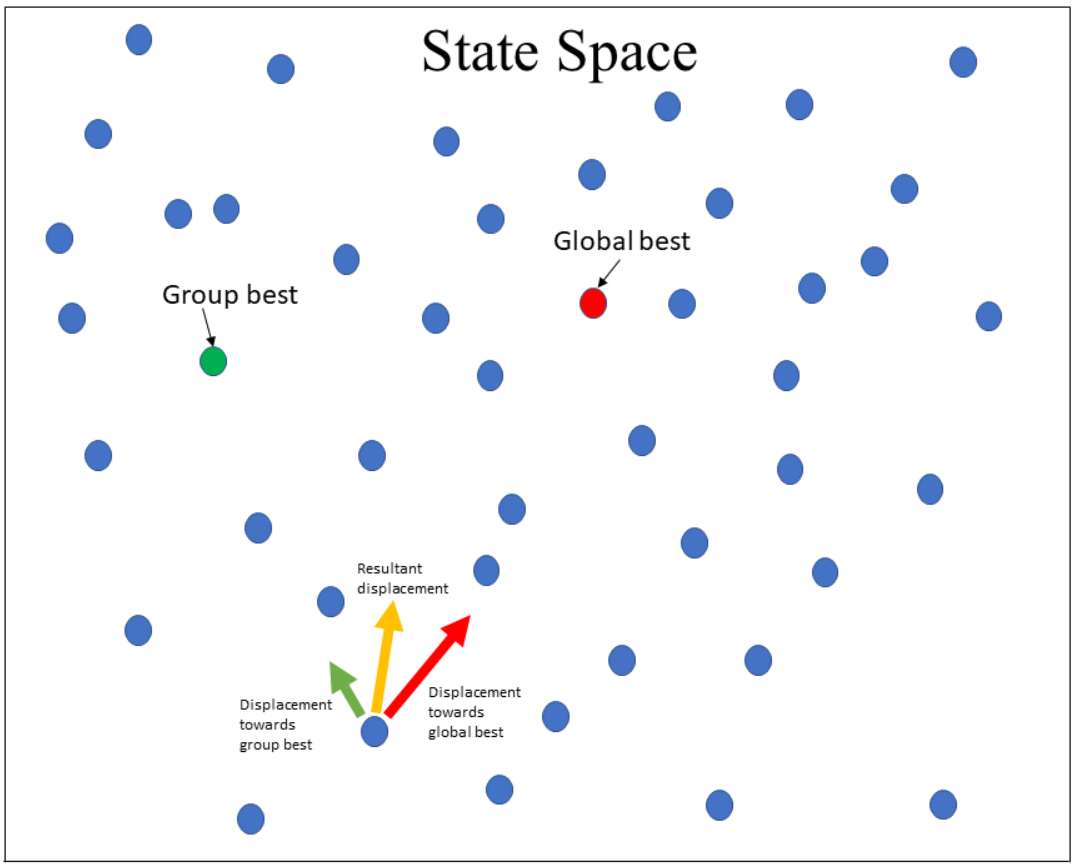

Figure 4: Resultant displacement of particles based on the locations of global best and group best.

The particles are re-evaluated with the cost function (present case time derivative of Lyapunov function) and a new group best, a global best values are allotted. Convergence criteria [27] is that, the distance between all particles to global maxima of that particular iteration must be less than er. If the convergence criteria is not met, then the particles undergo displacement again by velocity function. In this way the particles explore the state space and ultimately converges to the global best (real maxima of the function). The parameters used in the PSO code is shown in Table 2. The domain for the optimization is taken as 0 to 10000 states in P, C_i, T_j and $\check{T}_j$ where i={1,...,6} and j={1,2,3}. Since, the normalized power and precursor concentrations are taken as state variables, all the above mentioned variables are lie within the range of the chosen domain $\mathbb{D}$.

The global maximum of the function for a particular demand power ($P_d = 2$) which is in terms of

Parameters	**Values**
N	10000
N_g	100
$\mathbb{D}$	(0, 10000)
c_1, c_2	0.1, 0.3
er	0.001

Table 2: PSO parameters used in the simulation.

relative power, with respect to number of iterations is plotted in Figure (5 a). The result shows that the maxima of the given cost function (equation (26)) is -0.0725.

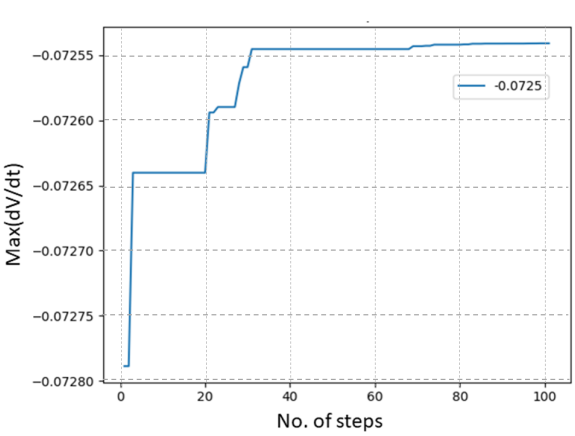

(a) Optimized result of PSO for a particular demand power ($P_d = 2$). Time derivative of Lyapunov function versus iteration steps

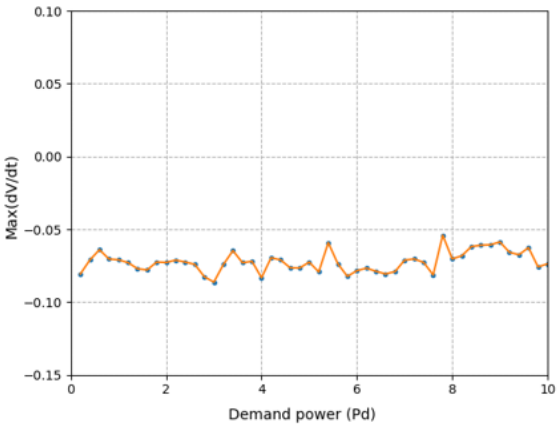

(b) Maximum value of time derivative of Lyapunov function with respect to demand power (P_d)

Figure 5: Plots for finding maxima of time derivative of Lyapunov function through particle swarm optimization

Similarly, the change in maxima of the time derivative of Lyapunov function with respect to change in demand power is shown in Figure (5 b). Though we have studied a wider range of relative power (0-10) is to demonstrate the robustness of controller's stability and also for the cliff edge studies. As per the plot, the function maxima remain negative. Hence we can conclude that $\dot{V}$ is negative definite and the considered nonlinear system (IDCC) is asymptotically stable in the domain $\mathbb{D}$.

4 Simulation and discussion

For comparative evaluation of the performance of IDCC with a robust nonlinear controller, SMC has been selected in addition to the standard PID controller. The following subsection presents an outline of the SMC for reactor power control.

4.1 Sliding mode controller

Sliding mode control is one of the popular nonlinear controls (also referred as variable structure control), which has inherent model error rejection and robust control characteristics. The SMC involves two steps [28]. In the first step, a sliding manifold is defined using the equation,

$$s\left(t\right) = \left(\frac{d}{dt} + q\right)^{r-1} e\left(t\right) = 0 \tag{29}$$

Where, q is a positive constant, r is the relative degree which is the minimum order of Lie derivative of output function of the dynamical system required for the control variable to appear explicitly, and e(t) is the tracking error. In the second step a control law is designed, so as to drive the system towards the sliding surface in finite time. This is done by defining the Lyapunov function $V\left(x\right) = \frac{1}{2}s^2$ and requiring that $\dot{V} < -\eta|s|$ or equivalently, $s\ \dot{s} < -\eta|s|$ and η is a strictly positive constant. A suitable function for the control rod reactivity (control input) $\rho_{cr}\left(t\right)$ is chosen to satisfy the Lyapunov condition. The resulting form of the control law is given below in equation (28).

$$\begin{aligned}\rho_{cr}\left(t\right) = \beta - \frac{\Lambda}{P\left(t\right)}\sum_{i=1}^{6}\beta_i C_i\left(t\right) + \frac{\Lambda}{P\left(t\right)}\frac{dP_d\left(t\right)}{dt} \\ -\frac{\Lambda}{P\left(t\right)}\eta\tanh\left(\frac{\left(P\left(t\right) - P_d\left(t\right)\right)}{\phi}\right) - \rho_f(t)\end{aligned} \tag{30}$$

Where, the notations are the same as in the previous sections. η and ϕ are positive constants. The reader is referred to [28] for details of the derivation of the control law.

4.2 Case-1: Comparison of tracking performance with a challenging demand profile

A challenging demand power profile is constructed as shown in the top section of Figure (6). The profile amplitudes range from 0.01 to 3 times the normalized power. The duration of the profile lasts for 50 seconds. The tracking performance of IDCC is compared with both SMC and PID. In the present case, the system has no model error and uncertainty. In the later sections model error and uncertainty are added.

The comparison of IDCC with PID is shown in the bottom section of Figure (6) for the power profile mentioned above. The simulation results show that the maximum error of SMC is about 75% at points where there is sharp change in power. Whereas IDCC is able to control and track the power profile very well with less than 1% deviation.

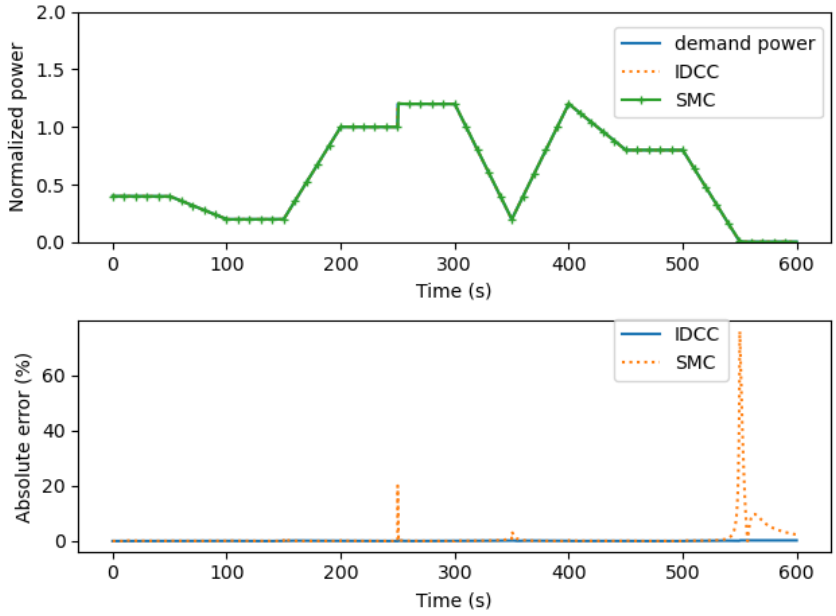

Figure 6: Performance comparison of IDCC with SMC. The plot shows the better control performance of IDCC compared with SMC to track the low power demand because of the low amplitude in the feedback signal.

The performance comparison of IDCC and manually tuned PID for the same power profile is shown in Figure (7). The simulated plots show that, PID has a maximum error of about 80% and moderate control ability in many fast varying sections of the demand power profile. Whereas the IDCC shows excellent performance with less than 1% deviation as discussed before.
The SMC and PID were unable to reach the low demand power in the order of 10^{-2} of P_d and having maximum error up to 80% because of the low amplitude in the feedback signal for low power cases whereas IDCC priory calculated the input required for any demand power with the help of feedforward unit, it able to control the power in high precision.

4.3 Case-2: Comparison of tracking performance with bounded uncertainty

In order to test the robustness of the IDCC in the presence of model error and bounded uncertainty, 10% error is added to the reactor parameter β and a noise signal of amplitude 0.5% of nominal power and frequency 2π Hz is added to the dynamics. Though feedforward controllers are inherently not able to handle the model discrepancies, since IDCC combines feedforward control with feedback control, it can easily handle model uncertainties.

The comparison of IDCC and SMC performance is shown in Figure (8). As per the simulation, the performance of SMC is slightly better than IDCC, because of its insensitivity to external noise and unmodeled dynamics. But the tracking performance of IDCC is not far off, which has a maximum error of about 2% and is still in the acceptable domain. The IDCC performance is also compared with a PID controller which is shown in the Figure (9). The maximum error when using PID controller is 4.5% but

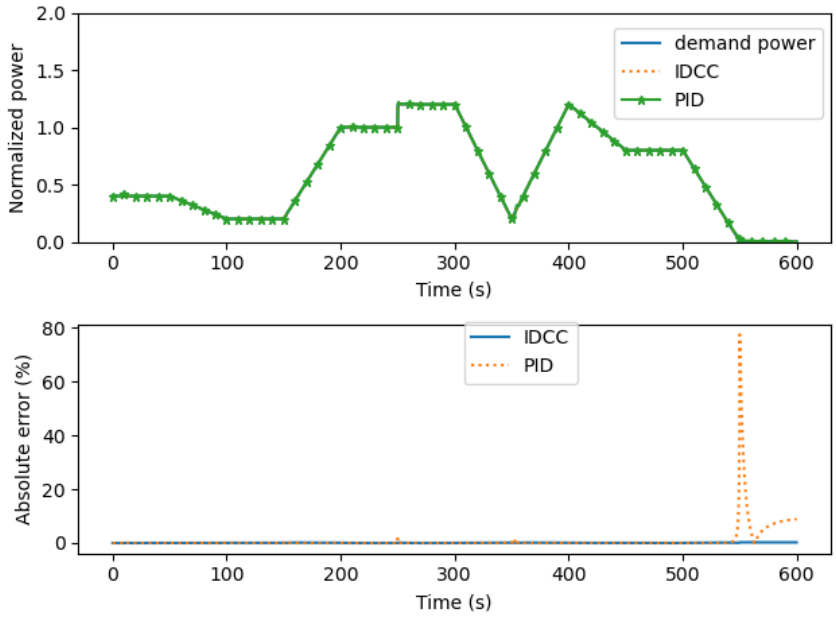

Figure 7: Performance comparison of IDCC with PID. The plot shows the better control performance of IDCC compared with PID to track the low power demand because of the low amplitude in the feedback signal.

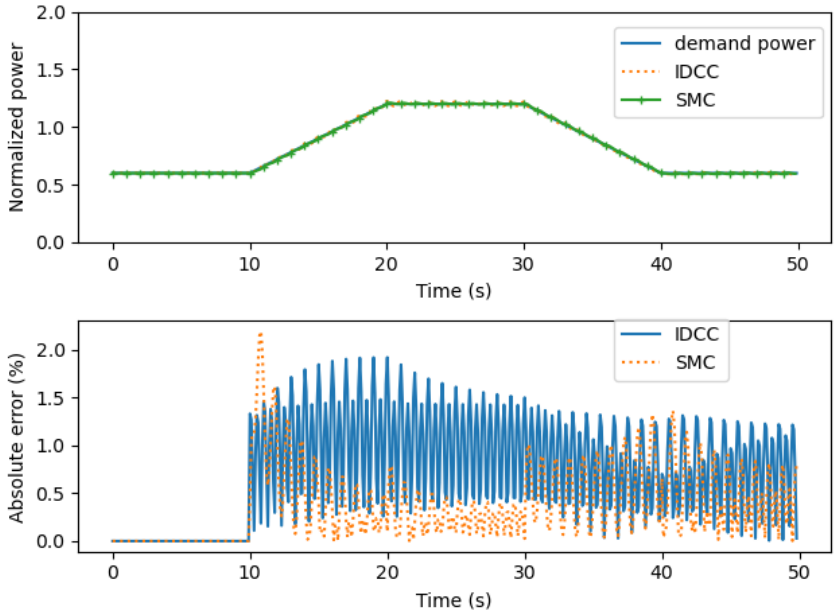

Figure 8: Performance of IDCC and SMC with model uncertainty. The Plot shows the inherent error tolerance behavior of SMC and the limited error handling ability of IDCC.

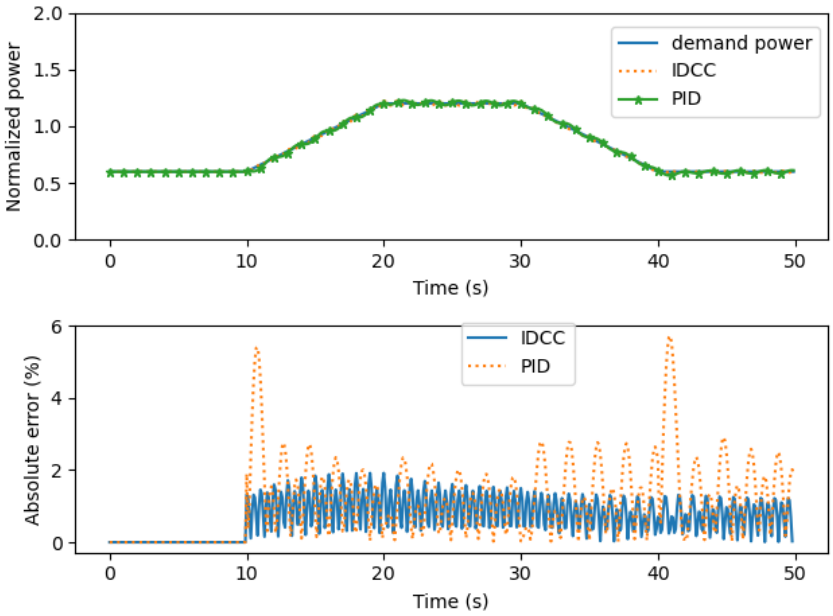

Figure 9: Performance of IDCC and PID with model uncertainty and noise. The PID can dampen the sinusoidal error introduced but it cannot anticipate the sudden change in demand, whereas IDCC has a limited ability to handle model uncertainties and large errors.

the maximum error with IDCC is only 2%. Since PID cannot anticipate sudden changes in demand, so there is more error whenever the demand profile changes. But PID can damp the sinusoidal noise introduced, whereas the IDCC has only a limited ability to suppress noise. Hence the performance of IDCC is better than the PID controller in the presence of model error and noise. The reactivity added by the feedforward module and the reactivity introduced by the PID controller of the IDCC is shown in the Figure (10). The responsibility of adding large reactivity gets delegated to the feedforward module, as indicated in the top graph of Figure (10). The reactivity corrections ρ_{pid} effected by the PID part of the IDCC, as shown in the lower graph remains less than about 30×10^{-5}, which is much less than the β (350×10^{-5}).

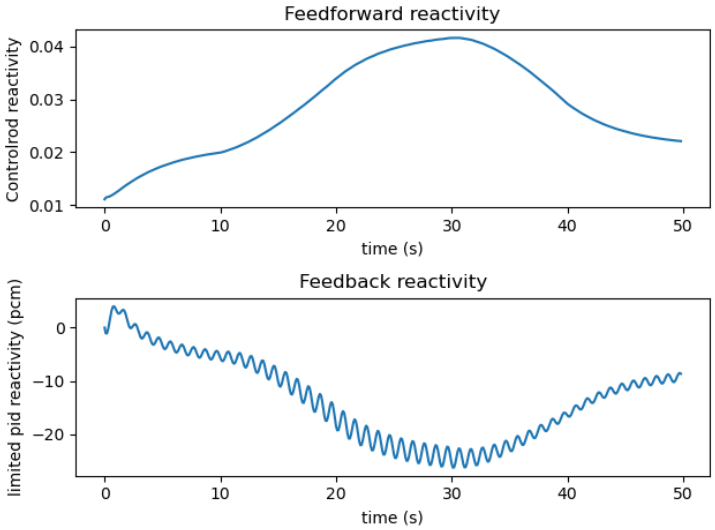

Figure 10: Reactivity plot of feedforward and feedback module of IDCC with model uncertainty and noise

4.4 Case-4: Fault tolerance

For this case, it is assumed in the simulation that, the power measurement signal is completely lost at time t = 30 seconds. The measured power signal can fail in at least three most likely modes, viz., failed indicating zero (stuck at zero), failed indicating maximum power (stuck at high) or stuck at some intermediate value when the reactor is operating at a nominal power. These failures can happen due to open or short circuit conditions, anywhere from the neutron detector to processing electronics, even in the presence of redundant configurations. Of these modes, the stuck at zero case is studied here, as this failure mode has the potential for driving the controlled power, to high unsafe values. This case is simulated with IDCC and compared with SMC and PID controllers, the results for which are shown in Figure (11). Though the IDCC is not able to track the demand power accurately, the deviation from the demand is within tolerable limit, but in the case of SMC and PID, the controllers drive the output power to unsafe levels. PID and SMC are not fault tolerant simply because these controllers are working with feedback signals. When the feedback signal is lost, these controllers can no longer control the system. As the error signal can diverge, leading to the divergence of output power. Though the performance level of IDCC with respect to robustness is not on par with SMC, it is clear from Figure (11) that it is has inherent fault tolerant capability with respect to the main tracked variable. It is to be noted that comparatively lesser robustness of IDCC is acceptable given its fault tolerance capability, which is more important in safety critical applications like nuclear reactor power control.

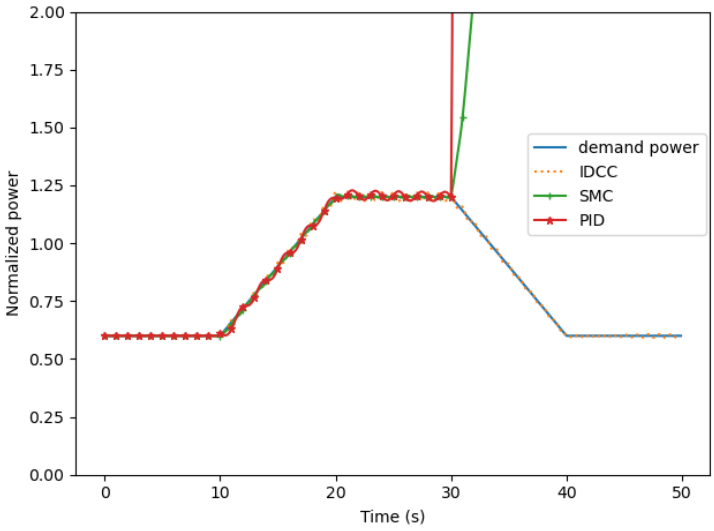

Figure 11: Performance of IDCC, SMC, and PID on power measurement failure. It is assumed that at 30^{th} second, the fault in the feedback signal has occurred.

5 Conclusion

A simple but fault tolerant and robust controller is designed, combining feedforward and feedback control schemes. Inverse dynamics is used to implement the feedforward part of the control to effect major corrections, while PID control is used for the reactivity limited feedback control to take care of uncertainty. The nonlinear stability analysis of proposed controller is examined using Lyapunov's direct method and the negative definiteness of time derivative of Lyapunov function is demonstrated with the help of particle swarm optimization technique. The performance of the combined IDCC is studied in comparison with a manually tuned PID controller and SMC. From the study, it is established that for controlling various challenging test power trajectories with model error and noise, the IDCC performs better than PID and is comparable to SMC. However, with respect to fault tolerance, it is demonstrated by a case study that the IDCC is tolerant to faults in the power measurement, though the robustness is marginally less compared to SMC. The limitations of the IDCC are the incapability to handle the unmodelled dynamics and system noise. Though it is fail-safe, it has a more complex algorithm compared to other controllers like SMC and PID. Further studies are in progress to establish the stability characteristics of proposed controller analytically and methods which incorporate fault tolerance in other measured variables, actuators are also being investigated.

Nomenclature

IDCC - Inverse Dynamics Corrected Control
NPP - Nuclear Power Plant
PID - Proportional Integral Derivative
SMC - Sliding Mode Control
SFR - Sodium-cooled Fast Reactor
LQR - Linear Quadratic Regulator
MPC - Model Predictive Control
IPKE - Inverse Point Kinetics Equation
PSO - Particle Swarm Optimization

References

[1] Abu-Khadar, Mazen M, "Recent advances in nuclear power: A review", Progress in Nuclear Energy, 51.2: 225-235 (2009).

[2] Marcin Karol Rowinski, Timothy John White, Jiyun Zhao, "Small and Medium sized Reactors (SMR): A review of technology", Renewable and Sustainable Energy Reviews, 44 643-656 (2015).

[3] Manfred Lenzen, "Life cycle energy and greenhouse gas emissions of nuclear energy: A review", Energy Conversion and Management, 49-8:2178-2199 (2008).

[4] Gang Li, X Wang, B Liang, X Li, B Zhang, Y Zou, "Modeling and control of nuclear reactor cores for electricity generation: A review of advanced technologies", Renewable and Sustainable Energy Review, 60:116-128 (2016).

[5] Defence in depth in nuclear safety – INSAG 10, Vienna, International Nuclear Safety Group, AIEA, (1996).

[6] Ehsan Hatami, H Salarieh, N Vosoughi, "Design of a fault tolerated intelligent control system for a nuclear reactor power control: Using extended Kalman filter", Journal of Process Control, 24:176-1084 (2014).

[7] EvrenEryurek, BR Upadhyaya, "Fault-tolerant control and diagnostics for large-scale", IEEE control systems, 15:534-42 (1995).

[8] Lynne M. Stevens, "Next generation nuclear plant resilient control system", Functional Analysis, 41:48, 188-199 (2017).

[9] M. Zarei, Reza Ghaderi, N. Kojuri, A. Minuchehr, "Robust PID control of power in lead cooled fastreactors; A direct synthesisframework", Annals of Nuclear Energy, 102:200-209 (2017).

[10] Mousakazemi, Seyed Mohammad Hossein, Navid Ayoobian, and Gholam Reza Ansarifar, "Control of the reactor core power in PWR using optimized PID controller with the real-coded DA", Annals of Nuclear Energy, 118:107-121 (2018).

[11] K. D. Young, V. I. Utkin and U. Ozguner, "A control engineer's guide to sliding mode control", IEEE Transactions on Control Systems Technology, 7-3:328-342 (1999).

[12] Park, Moon Ghu and Nam Zin Cho, "Time-optimal control of nuclear reactor power with adaptive proportional-integral-feedforward gains", IEEE Transactions on Nuclear Science, 40.3: 266-70 (1993).

[13] Guoxu Wang, J Wu, B Zeng, Z Xu, W Wu, X Ma, "Design of a model predictive control method forload tracking in nuclear power plants", Progress in Nuclear Energy, 101:260-269 (2017).

[14] Gang Li, "Modeling and LQG/LTR control for power and axial power difference of load-follow PWR core", Annals of Nuclear Energy, 68:193-203 (2014).

[15] Langewiesche, William, "What really brought down the Boeing 737Max", The New York Times Magazine, 18 (2019).

[16] Zhao, Yangping, Robert M. Edwards, and Kwang Y. Lee, "Hybrid feedforward and feedback controller design for nuclear steam generators over wide range operation using genetic algorithm", IEEE Transactions on Energy Conversion, 12.1: 100-105 (1997).

[17] Shaffer, Roman, Weidong He, and Robert M. Edwards, "Design and validation of optimized feedforward with robust feedback control of a nuclear reactor", Nuclear technology, 147.2: 240-257 (2004).

[18] MogensBlanke, W. Christian Frei, Franta Kraus, J. Ron Patton, Marcel Staroswiecki, "What is fault-tolerant control?", IFAC Proceedings Volumes, 33.11: 41-52, (2000).

[19] Xin Jin, Asok Ray, Robert M. Edwards, "Integrated robust and resilient control of nuclear power plants for operational safety and high performance", IEEE Transactions on Nuclear Science, 57(2):807-817 (2010).

[20] 20. Jeffery Lewins,"Nuclear Reactor Kinetics and Control", 1st edition, Elsevier (2013).

[21] Rafiei, M., G. R. Ansarifar, K. Hadad, and M. Mohammadi. "Load-following control of a nuclear reactor using optimized FOPID controller based on the two-point fractional neutron kinetics model considering reactivity feedback effects." Progress in Nuclear Energy 141 (2021): 103936.

[22] Arda, Samet E., and Keith E. Holbert. "Nonlinear dynamic modeling and simulation of a passively cooled small modular reactor." Progress in Nuclear Energy 91 (2016): 116-131.

[23] R. C. Berkan, B R Upadhyaya, L H Tsoukalas, "Reconstructive inverse dynamics control and application to xenon-induced power oscillations in pressurized water reactors", Nuclear Science and Engineering, 109:2,188-199 (2017).

[24] Ball, Thomas A, "The inverse kinetics method and its application to the annular core research reactor", Master of Science (Nuclear Engineering) Thesis, The University of New Mexico Albuquerque, New Mexico, (2017).

[25] David L. Hetrick, "Chapter 7- Nonlinear system stability", Dynamics of nuclear reactors, The University of Chicago press, (1971).

[26] Xin-She Yang, "Chapter 8 - Particle Swarm Optimization", Nature-Inspired Optimization Algorithms (Second Edition), Academic Press, Pages 111-121, (2021).

[27] Ioan Cristian Trelea, "The particle swarm optimization algorithm: convergence analysis and parameter selection", Information Processing Letters, Volume 85, Issue 6, Pages 317-325, ISSN 0020-0190, (2003).

[28] Ansarifar G. R., Saadatzi S, "Sliding mode control for pressurized-water nuclear reactors in load following operations with bounded xenon oscillations", Annals of Nuclear Energy, 76, 209–217 (2015).